

Functional Specialization of Neural Input Elements to the *Drosophila* ON Motion Detector

Highlights

- Medulla cells Mi1 and Tm3 are involved in the detection of ON motion
- Mi1 is a necessary element over all contrasts, velocities, and directions
- Tm3 is specialized in the computation of fast ON motion signals
- The effect of blocking Tm3 is direction dependent

Authors

Georg Ammer, Aljoscha Leonhardt,
Armin Bahl, Barry J. Dickson,
Alexander Borst

Correspondence

gammer@neuro.mpg.de (G.A.),
aborst@neuro.mpg.de (A.B.)

In Brief

Ammer et al. investigate the function of *Drosophila* medulla cells Mi1 and Tm3 in ON motion detection. They find that Mi1 is a necessary element over all stimulus conditions. Tm3, in contrast, plays a more specialized role, being specifically involved in the detection of fast movement in the preferred direction.

Functional Specialization of Neural Input Elements to the *Drosophila* ON Motion Detector

Georg Ammer,^{1,*} Aljoscha Leonhardt,¹ Armin Bahl,^{1,3} Barry J. Dickson,² and Alexander Borst^{1,*}

¹Max Planck Institute of Neurobiology, Am Klopferspitz 18, 82152 Martinsried, Germany

²Janelia Research Campus, Howard Hughes Medical Institute, 19700 Helix Drive, Ashburn, VA 20147, USA

³Present address: Department of Molecular and Cell Biology, Harvard University, 16 Divinity Avenue, Cambridge, MA 02138, USA

*Correspondence: ammer@neuro.mpg.de (G.A.), aborst@neuro.mpg.de (A.B.)

<http://dx.doi.org/10.1016/j.cub.2015.07.014>

SUMMARY

Detecting the direction of visual movement is fundamental for every sighted animal in order to navigate, avoid predators, or detect conspecifics. Algorithmic models of correlation-type motion detectors describe the underlying computation remarkably well [1–3]. They consist of two spatially separated input lines that are asymmetrically filtered in time and then interact in a nonlinear way. However, the cellular implementation of this computation remains elusive. Recent connectomic data of the *Drosophila* optic lobe has suggested a neural circuit for the detection of moving bright edges (ON motion) with medulla cells Mi1 and Tm3 providing spatially offset input to direction-selective T4 cells, thereby forming the two input lines of a motion detector [4]. Electrophysiological characterization of Mi1 and Tm3 revealed different temporal filtering properties and proposed them to correspond to the delayed and direct input, respectively [5]. Here, we test this hypothesis by silencing either Mi1 or Tm3 cells and using electrophysiological recordings and behavioral responses of flies as a readout. We show that Mi1 is a necessary element of the ON pathway under all stimulus conditions. In contrast, Tm3 is specifically required only for the detection of fast ON motion in the preferred direction. We thereby provide first functional evidence that Mi1 and Tm3 are key elements of the ON pathway and uncover an unexpected functional specialization of these two cell types. Our results thus require an elaboration of the currently prevailing model for ON motion detection [6, 7] and highlight the importance of functional studies for neural circuit breaking.

RESULTS

A large number of studies provide strong evidence that motion vision in flies is based on correlation-type motion detectors (Figure 1A) [8–12]. In recent years, great progress has been made in revealing the internal structure and identifying some of the cellular elements constituting the *Drosophila* motion-detection

circuit [13, 14]. In particular, it was shown that motion detection occurs in two parallel pathways that differ with respect to their preference for moving brightness increments (ON pathway) and brightness decrements (OFF pathway) [15, 16]. Genetic approaches to specifically silence neuronal cell types combined with electrophysiological and behavioral measurements have mainly focused on lamina circuits and identified cells that feed into the ON or OFF pathway, or both [15, 17–19]. T4 and T5 cells were discovered as the first cells in the *Drosophila* visual system that are direction selective and represent the output stages of ON and OFF elementary motion detectors, respectively [20]. Medulla cells that relay information from the lamina to the dendrites of T4 and T5 have been characterized anatomically [4, 21, 22] and, in part, electrophysiologically [5] or by calcium imaging [23, 24]. However, the functional role of medulla cells in generating direction-selective responses in postsynaptic T4 or T5 cells is still unknown. In this study, we focus on two medulla cell types of the ON pathway: Mi1 and Tm3. These two cell types form the great majority of synaptic inputs to T4 cells (Figure 1B) [4] and exhibit different temporal filtering properties [5]. Thus, it has been proposed that Mi1 and Tm3 constitute the delayed and direct input lines of the *Drosophila* ON motion detector, respectively (Figure 1C) [4, 5]. Here, we test this hypothesis experimentally.

A Candidate Circuit for ON Motion Detection

We first generated a simple computational model for a fully opponent correlation-type motion detector that computes ON and OFF motion in separate channels [25]. To test the functional role of the individual input elements, we simulated their removal from the circuit by setting their output gain to zero and computed the response of the detector. As expected, when we blocked either of the two input arms of the ON channel, the detector lost its direction selectivity for ON motion completely (Figure 1D). This model thus generates a clear prediction for our subsequent physiological and behavioral investigations: if Mi1 and Tm3 indeed constitute the two input lines of the ON motion detector, then functionally silencing either of them should lead to a complete loss of direction-selective responses to moving ON stimuli in downstream circuits and behavior under all stimulus conditions.

Mi1 Is an Essential Element of the ON Motion Vision Pathway

In order to measure the output of the motion-detection circuit, we performed *in vivo* patch-clamp recordings from direction-selective lobula plate tangential cells, which receive input from

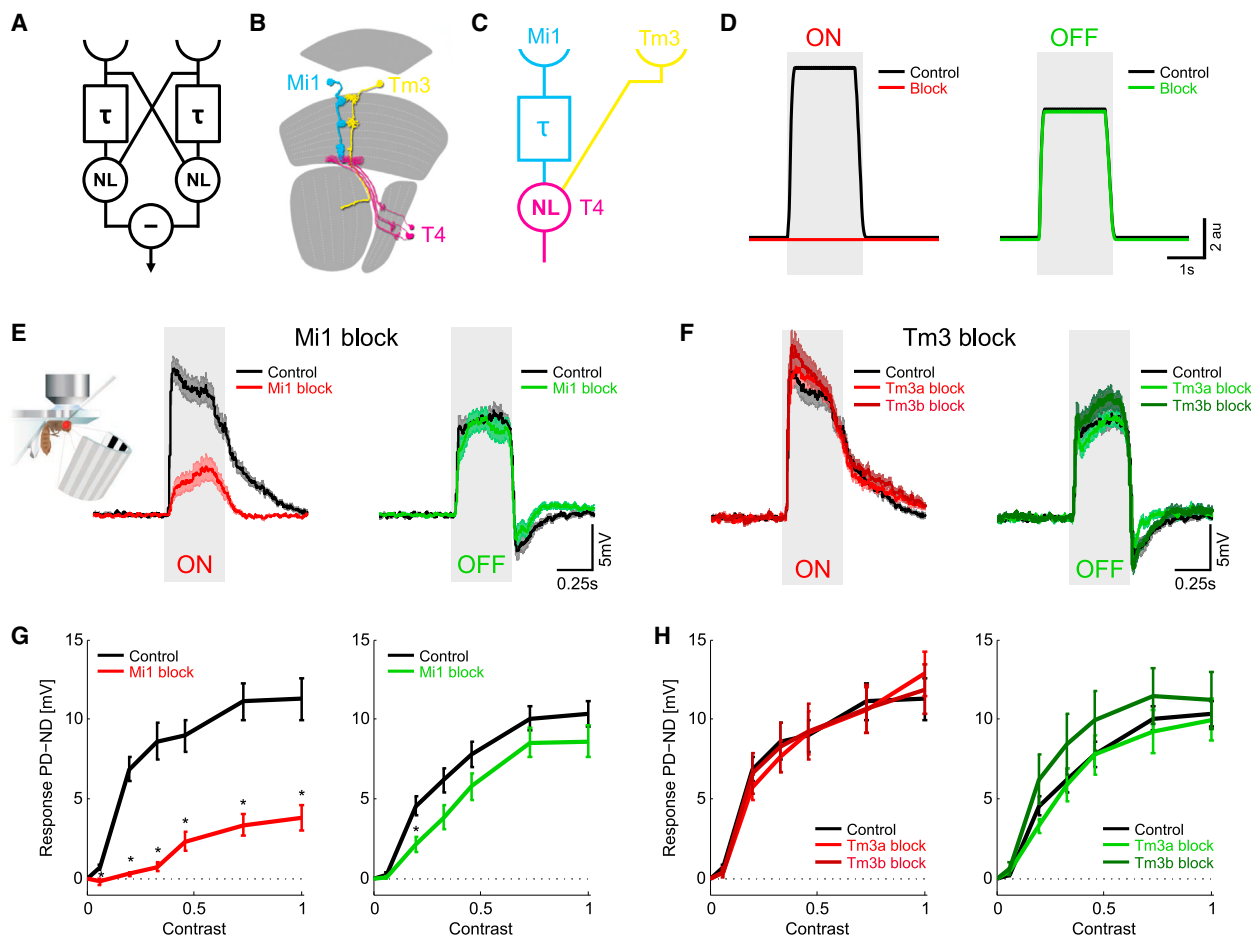


Figure 1. Voltage Responses of Lobula Plate Tangential Cells in Mi1 and Tm3 Block Flies

(A) Correlation-type motion detector. Two spatially separated input lines interact in a nonlinear way after one of them has been temporally delayed. Two mirror-symmetrical subunits are subtracted to yield a fully opponent direction-selective response.

(B) Anatomy of the neural input elements to T4 cells. Mi1 (cyan) and Tm3 (yellow) are the cells with the strongest input to direction-selective T4 cells (magenta).

(C) Schematic model suggesting that Mi1 and Tm3 form the delayed and non-delayed arm of a motion detector. The nonlinearity occurs in T4 cells.

(D) Response of a computational simulation of correlation-type motion detectors when removing either the delayed or the direct line. With both input lines intact,

the detector produces direction-selective responses to both moving ON and OFF edges (black).

Blocking either of the two input lines of the ON channel abolishes

responses to ON motion (red) while leaving OFF motion (green) responses intact.

(E and F) Voltage responses of lobula plate tangential cells (calculated by subtracting the response for null direction [ND] stimulation from the response to preferred direction [PD] stimulation) to moving ON or OFF edges when Mi1 cells (E) or Tm3 cells (F) are silenced. Responses of control flies are depicted in black and of Mi1 or Tm3 block flies in red for ON motion and green for OFF motion (control, n = 16; Mi1 block, n = 21; Tm3a block, n = 23; Tm3b block, n = 20).

(G and H) Contrast dependence of lobula plate tangential cells to moving ON or OFF edges of Mi1 (G) and Tm3 (H) block flies. Control flies are depicted in black and block flies in red for ON and green for OFF motion stimuli. Null direction responses were subtracted from preferred direction responses (PD – ND)

(control, n = 12; Mi1 block, n = 14; Tm3a block, n = 9; Tm3b block, n = 10).

Data are presented as mean \pm SEM. n indicates the number of recorded cells. Significant differences between control and block flies are indicated by asterisks (two-sided Student's t test, Benjamini-Hochberg corrected, *p < 0.05). Detailed statistics are provided in Table S2. Recordings from vertical system (VS) and horizontal system (HS) cells were pooled. See also Figures S1 and S2 and Table S1.

a large number of T4 and T5 cells [26, 27], and stimulated flies with visual motion on an LED arena [9]. To silence the neuronal activity of Mi1 or Tm3 cells, we used the Gal4/UAS system [28] to specifically express the EGFP-tagged inward-rectifying potassium channel Kir2.1 [29]. We generated a specific SplitGal4 line [30] to target Mi1 cells and used two independent Gal4 lines for manipulation of Tm3 cells [31]. All transgenic lines showed clear expression of the Kir2.1 channel in the respective cell types when stained with antibodies against the EGFP tag (Figure S1). We selectively stimulated the ON and OFF motion vision path-

ways with either multiple ON or OFF edges moving in the same direction at a velocity of 50° s^{-1} . Control flies responded with strong direction-selective responses to both moving ON and OFF edges (Figures 1E and 1F). In contrast, Mi1 block flies showed a strong reduction in response to ON motion but were unaffected for OFF motion (Figure 1E). Thus, in accordance with the predictions from the proposed model [4, 5], Mi1 is an essential element of the ON motion pathway. Surprisingly however, when we blocked Tm3 cells, responses to both ON and OFF stimuli were indistinguishable from those of control flies

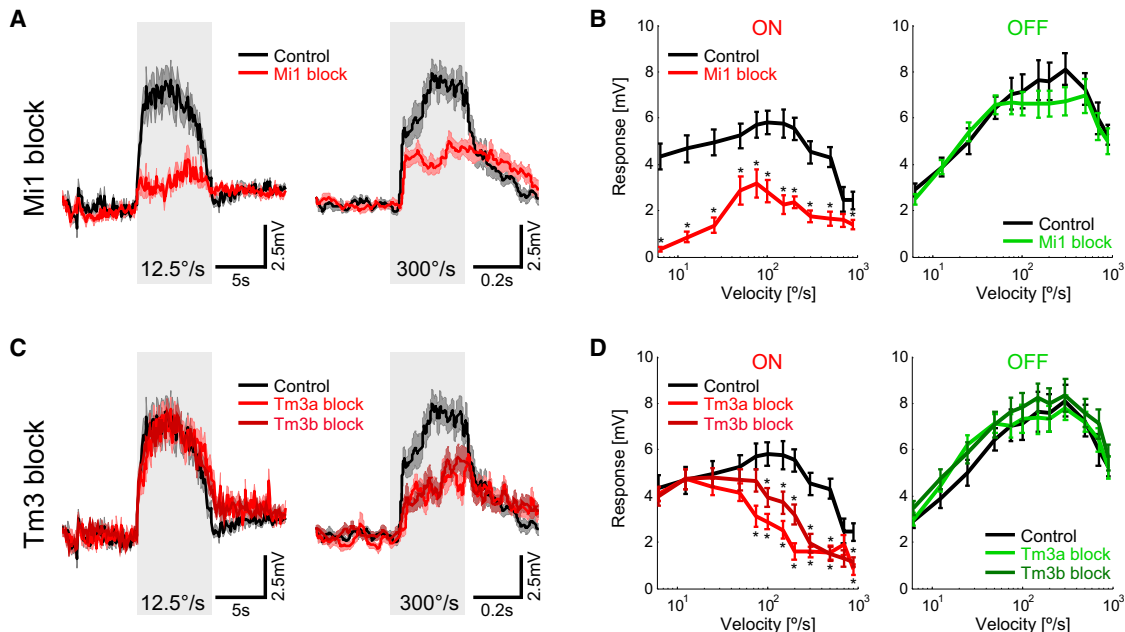


Figure 2. Differential Velocity Tuning of Mi1 and Tm3 Block Flies

(A) Average voltage responses of lobula plate tangential cells of control (black) and Mi1 block flies (red) to slow ($12.5^{\circ} \text{ s}^{-1}$) and fast ($300^{\circ} \text{ s}^{-1}$) ON edges moving in the preferred direction.

(B) Velocity tuning curves of lobula plate tangential cells of control (black) and Mi1 block flies to ON edges (red) and OFF edges (green) moving in the preferred direction (control, n = 13; Mi1 block, n = 11).

(C) Average voltage responses of lobula plate tangential cells of control (black) and Tm3 block (red) flies to slow ($12.5^{\circ} \text{ s}^{-1}$) and fast ($300^{\circ} \text{ s}^{-1}$) ON edges moving in the preferred direction.

(D) Velocity tuning curves of lobula plate tangential cells of control (black) and Tm3 block flies to ON edges (red) and OFF edges (green) moving in the preferred direction (control, n = 13; Tm3a block, n = 15; Tm3b block, n = 17).

Data are presented as mean \pm SEM. n indicates the number of recorded cells. Significant differences between control and block flies are indicated by asterisks (two-sided Student's t test, Benjamini-Hochberg corrected, *p < 0.05). Detailed statistics are provided in Table S2. Recordings from VS and HS cells were pooled. See also Figures S1 and S3 and Table S1.

(Figure 1F). To rule out that the strong stimulus drives the system to saturation and that possible residual Tm3 activity was sufficient to generate the observed responses, we varied the stimulus strength by reducing the contrast. Compared to control flies, Mi1 block flies showed a strong reduction to ON stimuli for all contrasts and a minor reduction to OFF stimuli in the low-contrast range (Figure 1G). However, responses of Tm3 block flies were again unaffected, even for very low contrasts (Figure 1H). Thus, we conclude, in disagreement with the proposed model [4, 5], that Tm3 cells are not necessary in general for the detection of ON motion.

Differential Velocity Dependence of Mi1 and Tm3 Block Flies

The finding that Tm3 is a dispensable circuit element under the tested stimulus conditions does not completely rule out its involvement in ON motion detection. It is possible that Tm3 plays an essential part under certain other stimulus conditions. In addition to the contrast tuning curve of a motion detector, another important characteristic is its dependence on velocity. We determined the velocity tuning curves by presenting single ON or OFF edges moving in the preferred direction at velocities that spanned two orders of magnitude. When blocking Mi1 cells, we found a strong response reduction for all velocities tested

(Figures 2A and 2B). The peak of the residual response was similar to that of control flies (Figure 2B). Flies in which Tm3 cells were silenced showed a drastically different phenotype: For slow velocities, responses were at control level, whereas responses to fast-moving ON edges were severely reduced (Figures 2C and 2D). The maxima of the ON tuning curves of Tm3 block flies were shifted to $12.5^{\circ} \text{ s}^{-1}$ and $25^{\circ} \text{ s}^{-1}$, respectively, as compared to $100^{\circ} \text{ s}^{-1}$ for control flies. For both Mi1 and Tm3 block flies, the responses to OFF motion remained at control levels. In conclusion, these experiments demonstrate that Tm3 cells are dispensable for the detection of slow ON edges but play a pivotal role in detecting fast ON motion.

Directionally Asymmetric Effect of Blocking Tm3 Cells

In addition to presenting edges moving in the preferred direction, we tested responses of Mi1 and Tm3 block flies to null direction stimulation. Control flies responded with a brief transient depolarization followed by a sustained hyperpolarization (Figure 3). For Mi1 block flies, we found a strong response reduction to moving ON edges over all tested velocities (Figures 3A and 3B). For high velocities, Mi1 block flies even showed a slight tonic depolarization, revealing an excitatory input that is largely masked in control flies. The source of this input is currently unknown but may be related to a T4/T5-independent

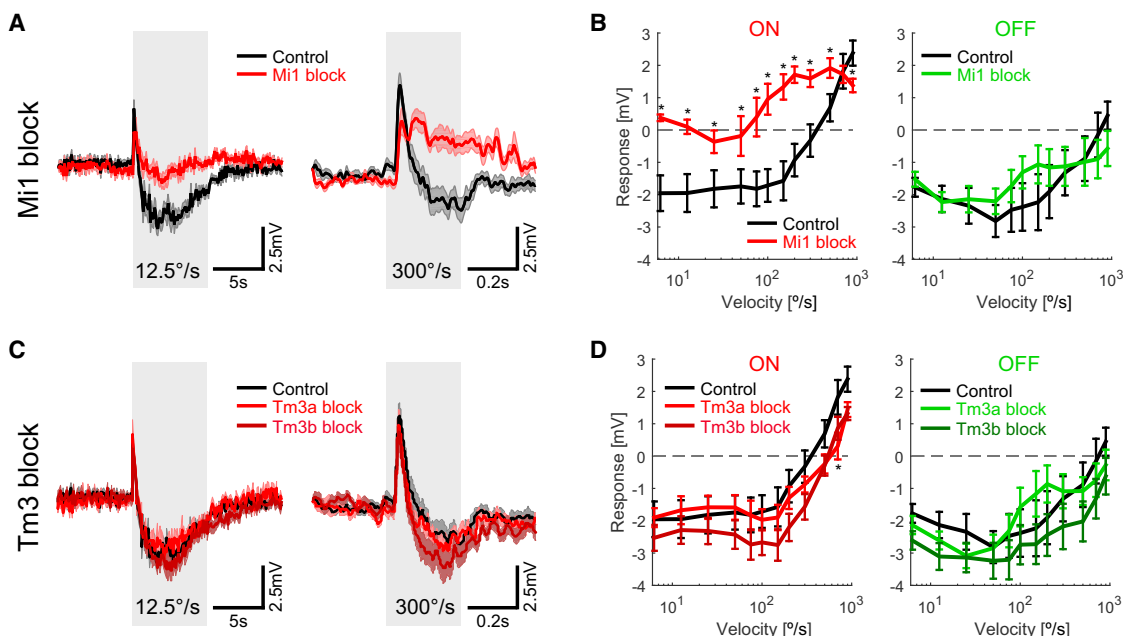


Figure 3. Voltage Responses of Lobula Plate Tangential Cells in Mi1 and Tm3 Block Flies to Edges Moving in the Null Direction

(A) Average voltage responses of lobula plate tangential cells of control (black) and Mi1 block flies (red) to slow ($12.5^{\circ} \text{ s}^{-1}$) and fast ($300^{\circ} \text{ s}^{-1}$) ON edges moving in the null direction.

(B) Velocity tuning curves of lobula plate tangential cells of control (black) and Mi1 block flies (red) to ON edges (red) and OFF edges (green) moving in the null direction (control, $n = 13$; Mi1 block, $n = 11$).

(C) Average voltage responses of lobula plate tangential cells of control (black) and Tm3 block (red) flies to slow ($12.5^{\circ} \text{ s}^{-1}$) and fast ($300^{\circ} \text{ s}^{-1}$) ON edges moving in the null direction.

(D) Velocity tuning curves of lobula plate tangential cells of control (black) and Tm3 block flies to ON edges (red) and OFF edges (green) moving in the null direction (control, $n = 13$; Tm3a block, $n = 15$; Tm3b block, $n = 17$).

Data are presented as mean \pm SEM. n indicates the number of recorded cells. Significant differences between control and block flies are indicated by asterisks (two-sided Student's t test, Benjamini-Hochberg corrected, $*p < 0.05$). Detailed statistics are provided in Table S2. Recordings from VS and HS cells were pooled. See also Figures S1 and S3 and Table S1.

flicker-sensitive pathway [27]. Responses to OFF motion were unaffected. Surprisingly, we did not find any effect of blocking Tm3 cells on responses to null direction motion (Figures 3C and 3D). Thus, the effect of blocking Tm3 cells is not only velocity dependent but is also dependent on the direction of stimulus motion.

Furthermore, we compared resting membrane potentials of control and Mi1 or Tm3 block flies (Table S1) and did not find significant differences. This suggests that a possible tonic synaptic transmission from Mi1 or Tm3 cells does not contribute significantly to the resting membrane potential of VS and HS cells, which otherwise might have influenced the amplitude of visual responses. Additionally, we did not observe any effect on magnitude, velocity tuning, or directional tuning of OFF motion responses for both Mi1 and Tm3 block flies (Figures 2 and 3), arguing for a strict separation of ON and OFF pathways at the level of Mi1 and Tm3.

Effects of Blocking Mi1 and Tm3 on Motion-Driven Behavior

In addition to the electrophysiological recordings from lobula plate tangential cells, we tested the functional contribution of Mi1 and Tm3 cells to motion-driven behaviors by blocking their synaptic output and measuring the turning responses of tethered

flies walking on an air-suspended ball [32, 33]. We used the temperature-sensitive silencing tool shibire^{ts} [34], which allowed us to block synaptic transmission conditionally by precisely controlling the ambient temperature in our behavioral setup. Thereby, we could rule out developmental effects that may have been caused by silencing Mi1 and Tm3 with Kir2.1 [29]. In order to test the differential impairment of ON and OFF motion channels, we used a balanced motion stimulus [19] and determined velocity tuning curves. This stimulus consists of multiple bright and dark edges moving simultaneously in opposite directions. Flies turn with the direction of moving edges [19]. Thus, wild-type flies with intact ON and OFF motion pathways are expected to show little or no turning responses, whereas flies with an impairment of the ON pathway turn with the direction of moving OFF edges and vice versa [19, 20]. Indeed, control flies showed only small turning responses for all velocities (Figures 4A–4D, black traces). Flies with silenced Mi1 cells, however, turned strongly with the direction of moving OFF edges, reflecting an impairment of the ON motion pathway in accordance with the electrophysiological experiments (Figure 4A). This was true for the whole range of tested velocities (Figure 4B). In contrast, Tm3 block flies showed only small turning responses to slowly moving edges but similarly strong responses as Mi1 block flies at high stimulus velocities (Figures 4C and 4D). The differential effect of silencing Mi1

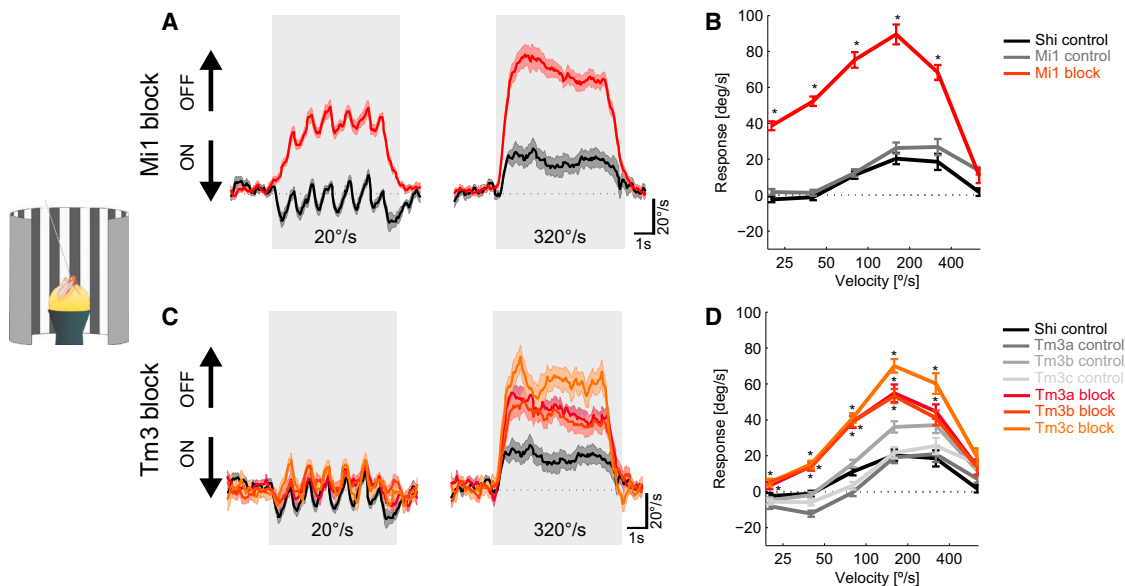


Figure 4. Behavioral Responses of Mi1 and Tm3 Block Flies

(A) Average turning speed of shibire control (black) and Mi1 block flies (red) to slow-moving ($20^{\circ} \text{ s}^{-1}$) and fast-moving ($320^{\circ} \text{ s}^{-1}$) opposing ON and OFF edges. Arrows at the left indicate the direction of moving ON and OFF edges.

(B) Velocity tuning curves for control (black and gray) and Mi1 block flies (red) to moving opposing edges (shibire control, n = 14; Mi1 control, n = 12; Mi1 block, n = 16).

(C) Average turning speed of shibire control (black) and Tm3 block flies (red) to slow-moving ($20^{\circ} \text{ s}^{-1}$) and fast-moving ($320^{\circ} \text{ s}^{-1}$) opposing ON and OFF edges. Arrows at the left indicate the direction of moving ON and OFF edges.

(D) Velocity tuning curves for control (black and gray) and Tm3 block flies (red) to moving opposing edges (shibire control, n = 14; Tm3a control, n = 12; Tm3b control, n = 12; Tm3c control, n = 13; Tm3a block, n = 12; Tm3b block, n = 15; Tm3c block, n = 12).

In (A) and (C), response traces of Gal4 controls were omitted for clarity. Data are presented as mean \pm SEM. n indicates the number of measured flies. Significant differences between both genotype controls and block flies are indicated by asterisks (two-sided Student's t test, Benjamini-Hochberg corrected, *p < 0.05). Detailed statistics are provided in Table S2. See also Figures S1 and S4.

and Tm3 was again strongest for low velocities and decayed for high velocities, as was seen before in the recordings from lobula plate tangential cells. The velocity range in which Mi1 and Tm3 block flies responded in a similar manner, however, was shifted to higher values compared to the electrophysiological measurements. This discrepancy is reminiscent of the difference in the temporal frequency optimum between lobula plate tangential cells and the optomotor response of walking flies [35] and is therefore likely to be due to the same mechanisms [36, 37]. The behavioral phenotype of Tm3 block flies resembles the preferred direction-specific effect that we observed in the electrophysiological experiments. It is currently unclear whether the hyperpolarization in tangential cells that is caused by null direction stimulation has a direct effect on the turning behavior of walking flies. Our results suggest that the depolarization that is induced by movement in the preferred direction is the dominant, if not the only force that drives turning behavior. Taken together, the findings from behavioral experiments are in agreement with the electrophysiological measurements and suggest a functional specialization of Mi1 and Tm3 cells with respect to their velocity-dependent input to T4 cells.

DISCUSSION

Direction-selective responses to moving bright edges first arise in T4 cells, but it is still unclear how these responses are shaped by T4's presynaptic inputs. Our results provide insight into this

question and demonstrate that Mi1 is an essential element for the detection of ON motion over all contrasts, velocity ranges, and directions of motion. This is consistent with Mi1 being one of the two input lines of an elementary motion detector. In contrast, Tm3 is dispensable under slow-motion stimulus conditions but necessary for the detection of fast movement in the preferred direction. Consequently, a Tm3-independent mechanism must exist that computes the direction of motion for slowly moving ON edges. Thus, ON motion is detected by at least two functionally specialized, complementary mechanisms: one detector for slow and another for fast motion, both sharing Mi1 cells as a common component. The combined action of these mechanisms allows the fly to detect visual motion over a larger range of velocities and more robustly. Additionally, modulatory or adaptive mechanisms would then be able to affect fast- and slow-motion-detection mechanisms independently.

Mechanistically, our findings give rise to two alternative hypotheses. First, Mi1 alone may be sufficient for generating direction-selective responses in T4 cells at slow velocities. In this scenario, the delay could be implemented by differential temporal filtering of Mi1 inputs that arrive at distal versus proximal locations of T4 cell dendrites. The asymmetric filtering may be due to the passive electrical properties of T4 cell dendrites which would impose a larger delay on signals arriving more distally, possibly in interaction with active dendritic conductances [38, 39]. This would offer a functional explanation for the finding that the anatomical orientation of T4 dendrites correlates with their

directional preference [4]. Indeed, such a role for dendritic morphology in conferring direction selectivity has been found in the Hb9⁺ subtype of retinal ganglion cells [40]. For these cells, compatible with our findings, dendritically mediated direction selectivity is only apparent at slow velocities, with inhibition-mediated direction selectivity dominating at high velocities. Alternatively, the delay may be implemented by Mi1 cells that have spatially offset receptive fields and target the same T4 cell dendrite but synapse onto receptors with different temporal transduction properties. Mi1 is reported to be cholinergic [41] and both fast nicotinic and slow muscarinic acetylcholine receptors are expressed in T4 cells [21]. These two scenarios would allow a single cell type (Mi1) to act as both the direct and delayed line, depending on the postsynaptic transduction mechanisms.

As a second hypothesis, additional inputs to T4 cells, other than Mi1 and Tm3, might be essential for the detection of ON motion at low velocities. Indeed, an ongoing connectomic study encompassing a larger volume of the medulla reports additional cells apart from Mi1 and Tm3 providing input to T4 cells (<http://emanalysis.janelia.org>). The strength of these newly described inputs was severely underestimated in the previous study [4], raising the possibility that they play an essential role in generating direction-selective signals in T4. Interestingly, such a scheme has recently been proposed for the OFF pathway, with Tm2 being the instantaneous input line of a motion detector that receives the delayed input from Tm1 and Tm9 cells, which are hypothesized to possess different temporal filtering characteristics [21]. Notably, for the first hypothesis, the delay needs to be implemented postsynaptically to Mi1, whereas the second hypothesis is compatible with a cell-intrinsic delay mechanism. Clearly, a definite understanding of the underlying cellular and biophysical mechanisms will require identification of the sign and temporal characteristics of all T4 synaptic inputs as well as blocking their synaptic output under different stimulus conditions.

Furthermore, our results revealed that the effect of blocking Tm3 cells is dependent on the direction of stimulus motion, with preferred direction responses being selectively affected. This directionally asymmetric effect is reminiscent of the behavioral phenotype that was observed when blocking certain subtypes of lamina cells [18]. Most interestingly, when blocking lamina cells C3, turning responses of tethered flying flies were selectively impaired only when presenting motion from back to front, but not from front to back. As an additional parallel to our Tm3 results, this effect was only present at high stimulus speeds [18]. C3 cells, as Mi1 and Tm3, receive strong input from lamina cells L1 and L5 and form, albeit few, input synapses to T4 [4]. The direction-dependent effect of blocking C3 cells was linked to wiring asymmetries of this cell type. Such an anatomical asymmetry has not yet been reported for Tm3 cells, as the directionality of wiring was not comprehensively analyzed in the recently published medulla connectome [4]. We hypothesize that such an anatomical asymmetry might exist and that it could account for the direction-dependent effect of blocking Tm3 cells that we observed.

In addition to the specific effects of blocking Mi1 or Tm3 on responses to ON motion, we found only a very mild effect on OFF responses. This suggests that Mi1 and Tm3, in contrast to many

lamina cells [17] and in agreement with an increase of rectification from distal to proximal medulla layers [24], feed almost exclusively into the ON pathway.

In conclusion, our study is the first functional demonstration that Mi1 and Tm3 cells are indeed crucial elements of the *Drosophila* ON motion detector, as previously suggested [4, 5]. However, while Mi1 is a necessary component under all stimulus conditions tested, the functionally segregated requirement of Tm3 with respect to stimulus velocity and direction suggests that additional yet unidentified cells or circuit mechanisms are involved as well.

SUPPLEMENTAL INFORMATION

Supplemental Information includes Supplemental Experimental Procedures, four figures, and two tables and can be found with this article online at <http://dx.doi.org/10.1016/j.cub.2015.07.014>.

AUTHOR CONTRIBUTIONS

G.A. and A. Borst designed the study. G.A. performed electrophysiological experiments and anatomical characterization of expression patterns, analyzed the data, and wrote the manuscript with the help of A. Borst, A.L., and A. Bahl. A.L. and A. Bahl performed behavioral experiments and analyzed data. B.J.D. generated SplitGal4 fly lines and hosted G.A. for characterization of Gal4 lines. A. Borst performed computational modeling.

ACKNOWLEDGMENTS

We thank Alexander Arenz and Jesus Pujol-Martí for critical comments on the manuscript, Etienne Serbe and Matthias Meier for many helpful discussions, Christian Theile and Romina Kutlesa for excellent help with behavioral experiments, and Wolfgang Essbauer and Michael Sauter for fly work. G.A., A.L., A. Bahl, and A. Borst are members of the Graduate School of Systemic Neurosciences (GSN) Munich.

Received: May 22, 2015

Revised: July 1, 2015

Accepted: July 2, 2015

Published: July 30, 2015

REFERENCES

- Hassenstein, B., and Reichardt, W. (1956). Systemtheoretische Analyse der Zeit-, Reihenfolgen- und Vorzeichenauswertung bei der Bewegungsperzeption des Ruesselkäfers *Chlorophanus*. Z. Naturforsch. B 11b, 513–524.
- Barlow, H.B., and Levick, W.R. (1965). The mechanism of directionally selective units in rabbit's retina. J. Physiol. 178, 477–504.
- Borst, A., and Euler, T. (2011). Seeing things in motion: models, circuits, and mechanisms. Neuron 71, 974–994.
- Takemura, S.Y., Bharoike, A., Lu, Z., Nern, A., Vitaladevuni, S., Rivlin, P.K., Katz, W.T., Olbris, D.J., Plaza, S.M., Winston, P., et al. (2013). A visual motion detection circuit suggested by *Drosophila* connectomics. Nature 500, 175–181.
- Behnia, R., Clark, D.A., Carter, A.G., Clandinin, T.R., and Desplan, C. (2014). Processing properties of ON and OFF pathways for *Drosophila* motion detection. Nature 512, 427–430.
- Plaza, S.M., Scheffer, L.K., and Chklovskii, D.B. (2014). Toward large-scale connectome reconstructions. Curr. Opin. Neurobiol. 25, 201–210.
- Takemura, S.Y. (2015). Connectome of the fly visual circuitry. Microscopy (Oxf.) 64, 37–44.
- Buchner, E. (1976). Elementary movement detectors in an insect visual system. Biol. Cybern. 24, 86–101.

9. Joesch, M., Plett, J., Borst, A., and Reiff, D.F. (2008). Response properties of motion-sensitive visual interneurons in the lobula plate of *Drosophila melanogaster*. *Curr. Biol.* 18, 368–374.
10. Götz, K.G. (1964). Optomotorische Untersuchung des visuellen Systems einiger Augenmutanten der Fruchtfliege *Drosophila*. *Kybernetik* 2, 77–92.
11. Götz, K.G. (1965). Die optischen Übertragungseigenschaften der Komplexaugen von *Drosophila*. *Kybernetik* 2, 215–221.
12. Schnell, B., Joesch, M., Forstner, F., Raghu, S.V., Otsuna, H., Ito, K., Borst, A., and Reiff, D.F. (2010). Processing of horizontal optic flow in three visual interneurons of the *Drosophila* brain. *J. Neurophysiol.* 103, 1646–1657.
13. Borst, A. (2014). In search of the Holy Grail of fly motion vision. *Eur. J. Neurosci.* 40, 3285–3293.
14. Silies, M., Gohl, D.M., and Clandinin, T.R. (2014). Motion-detecting circuits in flies: coming into view. *Annu. Rev. Neurosci.* 37, 307–327.
15. Joesch, M., Schnell, B., Raghu, S.V., Reiff, D.F., and Borst, A. (2010). ON and OFF pathways in *Drosophila* motion vision. *Nature* 468, 300–304.
16. Joesch, M., Weber, F., Eichner, H., and Borst, A. (2013). Functional specialization of parallel motion detection circuits in the fly. *J. Neurosci.* 33, 902–905.
17. Silies, M., Gohl, D.M., Fisher, Y.E., Freifeld, L., Clark, D.A., and Clandinin, T.R. (2013). Modular use of peripheral input channels tunes motion-detecting circuitry. *Neuron* 79, 111–127.
18. Tuthill, J.C., Nern, A., Holtz, S.L., Rubin, G.M., and Reiser, M.B. (2013). Contributions of the 12 neuron classes in the fly lamina to motion vision. *Neuron* 79, 128–140.
19. Clark, D.A., Bursztyn, L., Horowitz, M.A., Schnitzer, M.J., and Clandinin, T.R. (2011). Defining the computational structure of the motion detector in *Drosophila*. *Neuron* 70, 1165–1177.
20. Maisak, M.S., Haag, J., Ammer, G., Serbe, E., Meier, M., Leonhardt, A., Schilling, T., Bahl, A., Rubin, G.M., Nern, A., et al. (2013). A directional tuning map of *Drosophila* elementary motion detectors. *Nature* 500, 212–216.
21. Shinomiya, K., Karuppudurai, T., Lin, T.Y., Lu, Z., Lee, C.H., and Meinertzhagen, I.A. (2014). Candidate neural substrates for off-edge motion detection in *Drosophila*. *Curr. Biol.* 24, 1062–1070.
22. Takemura, S.Y., Karuppudurai, T., Ting, C.Y., Lu, Z., Lee, C.H., and Meinertzhagen, I.A. (2011). Cholinergic circuits integrate neighboring visual signals in a *Drosophila* motion detection pathway. *Curr. Biol.* 21, 2077–2084.
23. Meier, M., Serbe, E., Maisak, M.S., Haag, J., Dickson, B.J., and Borst, A. (2014). Neural circuit components of the *Drosophila* OFF motion vision pathway. *Curr. Biol.* 24, 385–392.
24. Strother, J.A., Nern, A., and Reiser, M.B. (2014). Direct observation of ON and OFF pathways in the *Drosophila* visual system. *Curr. Biol.* 24, 976–983.
25. Eichner, H., Joesch, M., Schnell, B., Reiff, D.F., and Borst, A. (2011). Internal structure of the fly elementary motion detector. *Neuron* 70, 1155–1164.
26. Mauss, A.S., Meier, M., Serbe, E., and Borst, A. (2014). Optogenetic and pharmacologic dissection of feedforward inhibition in *Drosophila* motion vision. *J. Neurosci.* 34, 2254–2263.
27. Schnell, B., Raghu, S.V., Nern, A., and Borst, A. (2012). Columnar cells necessary for motion responses of wide-field visual interneurons in *Drosophila*. *J. Comp. Physiol. A Neuroethol. Sens. Neural Behav. Physiol.* 198, 389–395.
28. Brand, A.H., and Perrimon, N. (1993). Targeted gene expression as a means of altering cell fates and generating dominant phenotypes. *Development* 118, 401–415.
29. Baines, R.A., Uhler, J.P., Thompson, A., Sweeney, S.T., and Bate, M. (2001). Altered electrical properties in *Drosophila* neurons developing without synaptic transmission. *J. Neurosci.* 21, 1523–1531.
30. Luan, H., Peabody, N.C., Vinson, C.R., and White, B.H. (2006). Refined spatial manipulation of neuronal function by combinatorial restriction of transgene expression. *Neuron* 52, 425–436.
31. Jenett, A., Rubin, G.M., Ngo, T.T., Shepherd, D., Murphy, C., Dionne, H., Pfeiffer, B.D., Cavallaro, A., Hall, D., Jeter, J., et al. (2012). A GAL4-driver line resource for *Drosophila* neurobiology. *Cell Rep.* 2, 991–1001.
32. Bahl, A., Ammer, G., Schilling, T., and Borst, A. (2013). Object tracking in motion-blind flies. *Nat. Neurosci.* 16, 730–738.
33. Seelig, J.D., Chiappe, M.E., Lott, G.K., Dutta, A., Osborne, J.E., Reiser, M.B., and Jayaraman, V. (2010). Two-photon calcium imaging from head-fixed *Drosophila* during optomotor walking behavior. *Nat. Methods* 7, 535–540.
34. Kitamoto, T. (2001). Conditional modification of behavior in *Drosophila* by targeted expression of a temperature-sensitive shibire allele in defined neurons. *J. Neurobiol.* 47, 81–92.
35. Chiappe, M.E., Seelig, J.D., Reiser, M.B., and Jayaraman, V. (2010). Walking modulates speed sensitivity in *Drosophila* motion vision. *Curr. Biol.* 20, 1470–1475.
36. Schnell, B., Weir, P.T., Roth, E., Fairhall, A.L., and Dickinson, M.H. (2014). Cellular mechanisms for integral feedback in visually guided behavior. *Proc. Natl. Acad. Sci. USA* 111, 5700–5705.
37. Suver, M.P., Mamiya, A., and Dickinson, M.H. (2012). Octopamine neurons mediate flight-induced modulation of visual processing in *Drosophila*. *Curr. Biol.* 22, 2294–2302.
38. Branco, T., Clark, B.A., and Häusser, M. (2010). Dendritic discrimination of temporal input sequences in cortical neurons. *Science* 329, 1671–1675.
39. Hausselt, S.E., Euler, T., Detwiler, P.B., and Denk, W. (2007). A dendrite-autonomous mechanism for direction selectivity in retinal starburst amacrine cells. *PLoS Biol.* 5, e185.
40. Trenholm, S., Johnson, K., Li, X., Smith, R.G., and Awatramani, G.B. (2011). Parallel mechanisms encode direction in the retina. *Neuron* 71, 683–694.
41. Hasegawa, E., Kitada, Y., Kaido, M., Takayama, R., Awasaki, T., Tabata, T., and Sato, M. (2011). Concentric zones, cell migration and neuronal circuits in the *Drosophila* visual center. *Development* 138, 983–993.

Current Biology

Supplemental Information

Functional Specialization of Neural Input Elements

to the *Drosophila* ON Motion Detector

Georg Ammer, Aljoscha Leonhardt, Armin Bahl, Barry J. Dickson, and Alexander Borst

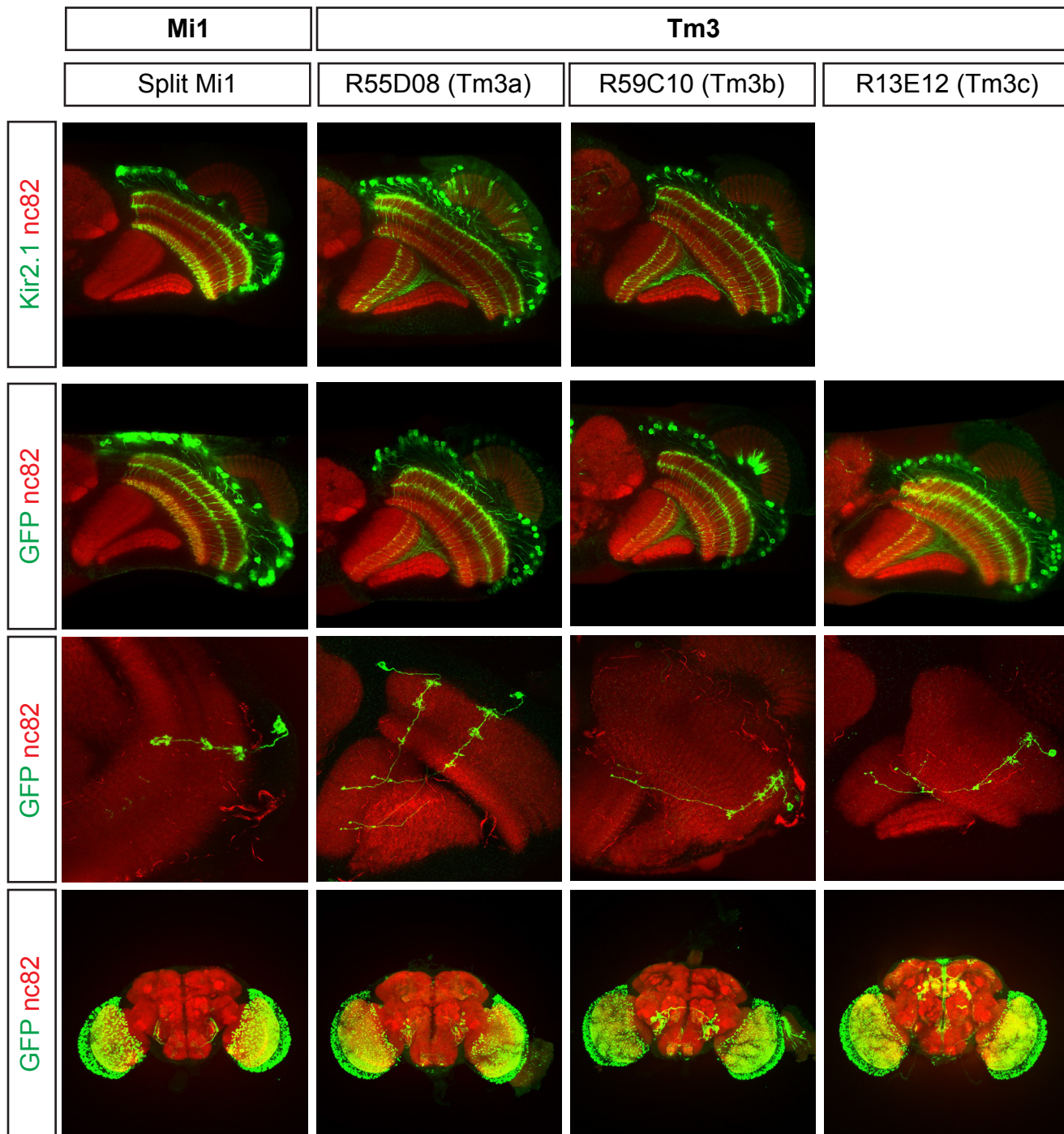


Figure S1 related to Figures 1-4: Expression Patterns of Gal4 Lines

Panels in the upper row show horizontal sections of brains dissected from flies with identical genotypes as in the electrophysiological experiments. Expression of Kir2.1 is visualized by staining for the EGFP tag that is fused to the Kir2.1-channel. Lower three panels show horizontal sections (top), single cell flip-outs (middle) and frontal sections (bottom) of brains of all fly lines used in this study. For characterization of expression patterns, UAS-GFP was driven by the respective Gal4 lines (see [Supplemental Experimental Procedures](#) for details).

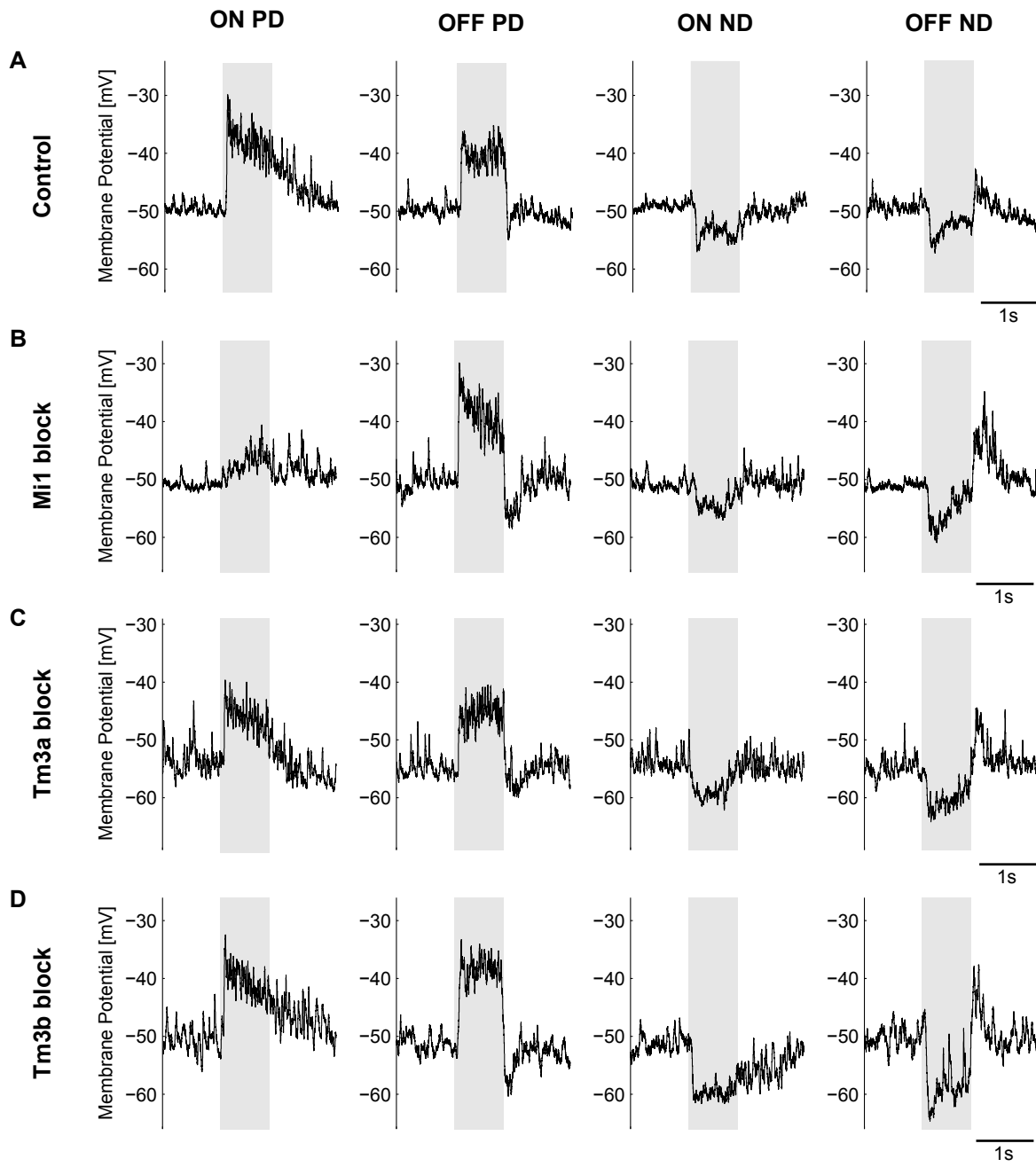


Figure S2 related to Figure 1: Representative Raw Voltage Traces of Control and Block Flies

Voltage responses of single VS or HS cells to multiple edges moving at a velocity of 50 °/s at full contrast. Traces are shown for ON and OFF edges moving in either the preferred direction (PD) or null direction (ND). (A) Single HS cell recording from a control fly. (B) Single HS cell recording from a Mi1 block fly. (C) Single HS cell recording from a Tm3a block fly. (D) Single VS cell recording from a Tm3b block fly. Grey shaded area indicates the stimulation period. Specific genotypes are listed in [Supplemental Experimental Procedures](#).

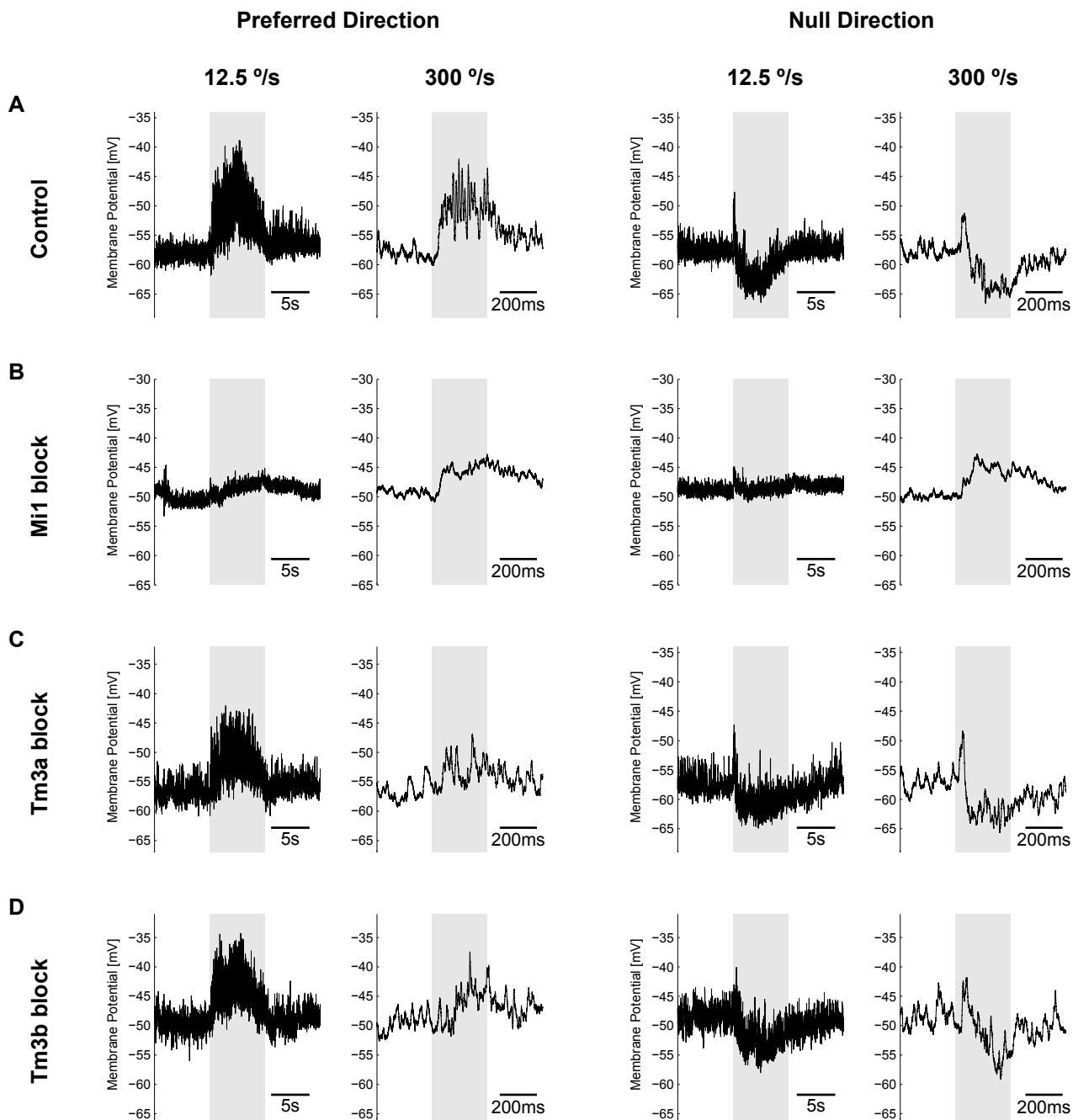


Figure S3 related to Figures 2 and 3: Representative Raw Voltage Traces of Control and Block Flies

Voltage responses of single VS or HS cells to single ON edges moving in the preferred direction (left panels) or null direction (right panels) at velocities of 12.5 °/s or 300 °/s at full contrast. (A) Single VS cell recording from a control fly. (B) Single VS cell recording from a Mi1 block fly. (C) Single VS cell recording from a Tm3a block fly. (D) Single VS cell recording from a Tm3b block fly. Grey shaded area indicates the stimulation period. Specific genotypes are listed in [Supplemental Experimental Procedures](#).

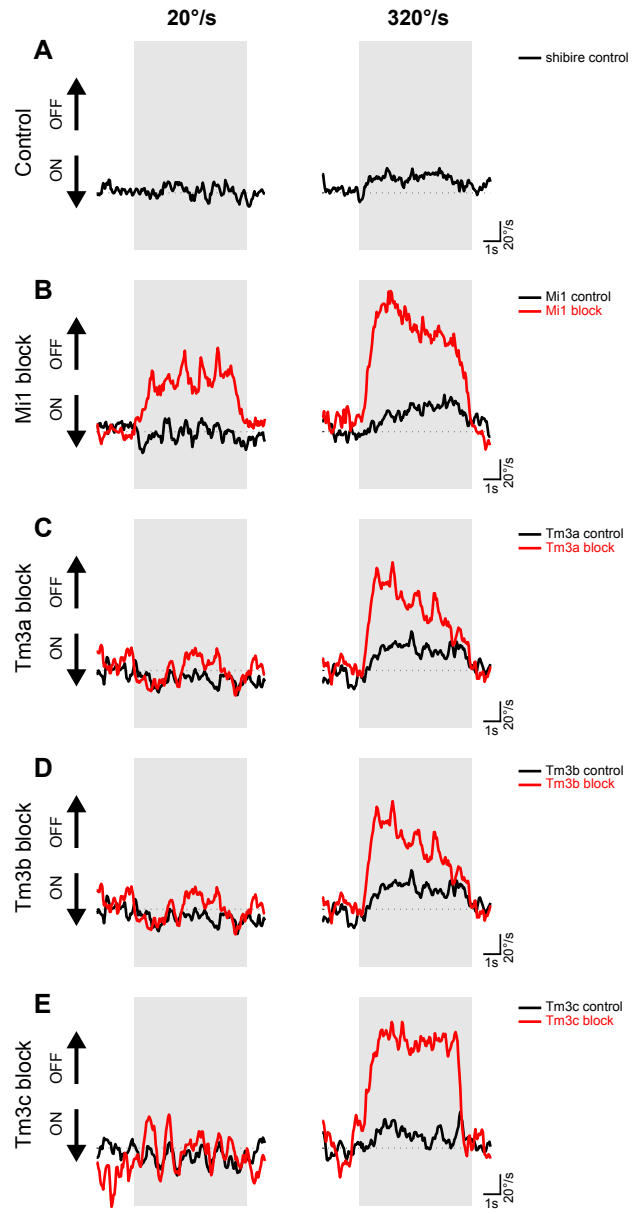


Figure S4 related to Figure 4: Representative Single Fly Responses of Control and Block Flies

Turning responses of single flies to multiple opposing edges moving at a velocity of either 20 °/s or 300 °/s. (A) Turning response of a single shibire control fly. (B) Turning response of a single Mi1 control fly (black) and Mi1 block fly (red). (C) Turning response of a single Tm3a control fly (black) and Tm3a block fly (red). (D) Turning response of a single Tm3b control fly (black) and Tm3b block fly (red). (E) Turning response of a single Tm3c control fly (black) and Tm3c block fly (red). Grey shaded area indicates the stimulation period. Specific genotypes are listed in [Supplemental Experimental Procedures](#).

Figure 1 E, F

Genotype	mean (mV)	s.e.m. (mV)	n (cells)
Control	-51.88	0.61	16
Mi1	-51.67	0.76	21
R55D08 (Tm3a)	-53.00	0.50	23
R59C10 (Tm3b)	-51.89	0.66	20

Figure 1 G, H

Genotype	mean (mV)	s.e.m. (mV)	n (cells)
Control	-51.75	0.65	12
Mi1	-51.64	0.63	14
R55D08 (Tm3a)	-53.44	0.69	9
R59C10 (Tm3b)	-51.75	0.98	10

Figure 2, 3

Genotype	mean (mV)	s.e.m. (mV)	n (cells)
Control	-51.58	0.81	13
Mi1	-51.50	0.70	11
R55D08 (Tm3a)	-52.07	0.52	15
R59C10 (Tm3b)	-52.06	0.71	17

Table S1 related to Figures 1-3: Resting Membrane Potentials of Lobula Plate Tangential Cells

Mean and s.e.m. of the resting membrane potentials of all recorded cells are listed. n denotes the number of recorded cells. Resting membrane potentials were corrected for a liquid junction potential of -12 mV. We did not find any statistically significant difference ($p < 0.05$) between controls and all tested genotypes when applying an unpaired two-sided Student's t-test. Specific genotypes are listed in [Supplemental Experimental Procedures](#).

Table S2 related to Figures 1-4: Detailed Statistics for all Figures

n-numbers, p-values and t-values for all statistical tests applied throughout the study. Statistical significance was tested by using a two-sided Student's t-test followed by a Benjamini-Hochberg correction (* p<0.05). Table S2 is supplied as a separate Excel spreadsheet.

Supplemental Experimental Procedures

Fly Stocks

Flies were reared on cornmeal agar medium under standard conditions (25° C, 60% humidity, 12hr dark/light cycle). For electrophysiology flies were used 5-30 hours post-eclosion. For behavioral experiments flies were aged 1-3 days. Only female flies were used in all experiments.

Genotypes of all fly strains used in the experiments:

Figures 1 - 3

$w^+ / w^- ; 10xUAS\text{-}Kir2.1\text{-}EGFP / + ; +$ (Control)

$w^+ / w^- ; 10xUAS\text{-}Kir2.1\text{-}EGFP / VT7747AD ; VT49371DBD / +$ (Mi1 block)

$w^+ / w^- ; 10xUAS\text{-}Kir2.1\text{-}EGFP / + ; R55D08\text{-}Gal4 / +$ (Tm3a block)

$w^+ / w^- ; 10xUAS\text{-}Kir2.1\text{-}EGFP / + ; R59C10\text{-}Gal4 / +$ (Tm3b block)

Figure 4

$w^+ / w^- ; 20xUAS\text{-}shibire^{ts} / + ; +$ (Shi control)

$w^+ / w^- ; VT7747AD / + ; VT49371DBD / +$ (Mi1 control)

$w^+ / w^- ; + / + ; R55D08\text{-}Gal4 / +$ (Tm3a control)

$w^+ / w^- ; + / + ; R59C10\text{-}Gal4 / +$ (Tm3b control)

$w^+ / w^- ; + / + ; R13E12\text{-}Gal4 / +$ (Tm3c control)

$w^+ / w^- ; 20xUAS\text{-}shibire^{ts} / VT7747AD ; VT49371DBD / +$ (Mi1 block)

$w^+ / w^- ; 20xUAS\text{-}shibire^{ts} / + ; R55D08\text{-}Gal4 / +$ (Tm3a block)

w⁺ / w⁻; 20xUAS-shibire^{ts} / +; R59C10-Gal4 / + (Tm3b block)

w⁺ / w⁻; 20xUAS-shibire^{ts} / +; R13E12-Gal4 / + (Tm3c block)

Figure S1

For analysis of expression patterns:

w⁺ / w⁻; UAS-mCD8-GFP, UAS-syt-HA / VT7747AD ; VT49371DBD / + (Mi1)

w⁺ / w⁻; UAS-mCD8-GFP, UAS-syt-HA / + ; R55D08-Gal4 / + (Tm3a)

w⁺ / w⁻; UAS-mCD8-GFP, UAS-syt-HA / + ; R59C10-Gal4 / + (Tm3b)

w⁺ / w⁻; UAS-mCD8-GFP, UAS-syt-HA / + ; R13E12-Gal4 / + (Tm3c)

For single cell flip-outs:

w⁻, pBPhsFlp2::PEST / w⁻; VT7747AD / +; VT49371DBD / UAS-FRT>>FRT-myr::GFP (Mi1)

w⁻, pBPhsFlp2::PEST / w⁻ ; + / + ; R55D08-Gal4 / UAS-FRT>>FRT-myr::GFP (Tm3a)

w⁻, pBPhsFlp2::PEST / w⁻ ; + / + ; R59C10-Gal4 / UAS-FRT>>FRT-myr::GFP (Tm3b)

w⁻, pBPhsFlp2::PEST/w⁻ ; + / + ; R13E12-Gal4 / UAS-FRT>>FRT-myr::GFP (Tm3c)

Immunohistochemistry and confocal microscopy

Antibody stainings were performed as previously described [S1]. We generated single cell flip-outs using a recently published method [S2]. Briefly, brains were dissected in PBS, fixed in 4% PFA (containing 0.1% Triton-X) for 25 min, washed 3x in PBT (PBS containing 0.3% Triton-X) and blocked with 10% NGS in PBT. Primary antibodies were diluted in PBT containing 5% NGS and incubated for 48 hrs at 4°C. After washing 3x in PBT, brains were incubated in secondary antibody solution for 48-72 hrs at 4°C. After washing 3x in PBT and 1x in PBS, brains were mounted in Vectashield (Vector labs). Following antibodies were used in this study:

Primary antibodies: rabbit anti-GFP (Torri Pines, 1:2000), mouse anti-nc82 (DSHB, 1:25); secondary antibodies: goat anti-rabbit 488 (Invitrogen, 1:500), goat anti-mouse 633 (Invitrogen, 1:500). Imaging was performed on a Leica SP5 confocal microscope with a 63x objective (HCx PL APO, 1.40 NA, Leica) for horizontal sections or a 20x objective (HC PL APO, 0.70 NA, Leica) for vertical sections at a resolution of 1024x1024. Images were processed in ImageJ 1.46f (NIH). Single z-slices are shown for horizontal views and maximum intensity projections for single cell flip-outs and frontal views.

Electrophysiology

Flies were anesthetized on ice, waxed to a plexiglas holder, inserted into an opening cut into aluminum foil and mounted in a recording chamber. A part of the posterior side of the head cuticle and the muscle that covers the cell bodies of LPTCs was removed with a needle and fine forceps. Extracellular saline (103 mM NaCl, 3 mM KCl, 5 mM TES, 10 mM trehalose, 10 mM glucose, 7 mM sucrose, 26 mM NaHCO₃, 1 mM NaH₂PO₄, 1.5 mM CaCl₂ and 4 mM MgCl₂, pH 7.3, 280 mOsm) was bubbled with 95% O₂ and 5% CO₂ and perfused over the preparation. The brain of the fly was visualized with an upright microscope (AxioTech Vario 100, Zeiss) equipped with a 40x water-immersion objective (LumPlanFL, NA 0.8, Olympus), an Hg-light source (HXP-120, Visitron Systems) and polarization filters for contrast enhancement. A glass electrode filled with collagenase (Collagenase IV, Gibco, 0.5 mg/ml in extracellular saline) was used to expose the somata of LPTCs. Somata of VS and HS cells were patched with a glass electrode (5–9 MΩ) filled with internal solution (140 mM potassium aspartate, 10 mM HEPES, 4 mM Mg-ATP, 0.5 mM Na-GTP, 1 mM EGTA, 1 mM KCl and 0.03 mM Alexa 568-hydrazide sodium, pH 7.26, 265 mOsm). Recordings were performed with an NPI BA-1S amplifier (NPI electronics) in

current-clamp bridge mode, low-pass filtered with a cut-off frequency at 3 kHz and digitized at 10 kHz. Data acquisition was performed with Matlab (version R2011a, MathWorks). Cell types were identified on the basis of their typical response profiles to moving gratings. In addition, the majority of recorded cells were dye filled and their identity verified anatomically.

Visual stimulation

Visual stimulation was performed with a custom-built LED arena that had dimensions of 170° in azimuth and 90° in elevation and a spatial resolution of approximately 1.4° per LED. The arena allowed refresh rates of up to 600 Hz and had a maximum luminance of 80 cd m⁻². Data analysis was performed with Matlab (version R2011b, MathWorks) using custom-written scripts. Multiple moving edges were presented as standing square wave gratings with a wavelength of 42°. During stimulation, either all the bright or all the dark edges of the grating moved at a velocity of 50° s⁻¹ for 0.45 s. To measure contrast tuning curves we varied the contrast of the gratings from 6% to 100% while keeping the mean luminance constant. To determine velocity tuning curves we used single edges at full contrast that covered at distance of 90° moving at the following velocities: 6.25, 12.5, 25, 50, 75, 100, 150, 200, 300, 500, 700 and 900 ° s⁻¹. Different velocities were presented in randomized order. Edges moved in the horizontal direction when recording from HS cells and in the vertical direction when recording from VS cells.

Data Analysis

For all stimuli, we averaged voltage traces during the whole stimulation period and calculated the mean and standard errors over cells.

Behavioral experiments

Flies were cold anesthetized before the experiment. Head, thorax, and wings were glued to a needle with near-UV bonding glue (Sinfony Opaque Dentin) and blue LED light (440 nm, dental curing-light, New Woodpecker). Flies were then placed on an air-suspended polyurethane ball in a virtual environment projected onto three monitors spanning approximately 270° (vertical) and 114° (horizontal) of the fly's visual field. This stimulation system offered less than 0.1° of angular pixel size, a value well below *Drosophila*'s optical resolution capability. We used six such setups for recording fly locomotion as described previously [S3]. On two setups, stimuli were presented at a screen refresh frequency of 120 Hz; on four setups, the refresh frequency was 144Hz. We never observed qualitative or quantitative differences between these setups in any of the experiments. All monitors were equilibrated in brightness and contrast. Temperature within the immediate surround of the fly was controlled using a custom-built closed-loop thermoregulation system. We employed the following temperature protocol for all experiments and genotypes: Temperature was kept at 25°C for the first 5 minutes and then, within 10 minutes, raised to a restrictive temperature of 34°C.

Visual Stimulation

Our balanced motion stimulus resembled the one used in previous studies [S4, S5]. Briefly, we presented flies with a stationary square wave grating that had an initial spatial wavelength of 45° visual angle and Michelson contrast of 50%. Each individual trial lasted 9s. Between 2s and 7s, bright edges moved in one direction at a fixed velocity while dark edges moved in the other direction at the same velocity. In contrast to previous versions, we reset the stimulus to the initial state after edges had traversed 20° of visual angle. This allowed us to keep the stimulus duration

fixed for varying edge velocities. Additionally, we applied a random phase shift after each reset in order to rule out symmetry effects. This was done for 6 velocities (20, 40, 80, 160, 320, and 640° s^{-1}) and 2 possible edge directions (dark edge leftwards/bright edge rightwards and vice versa), resulting in 12 conditions that were repeated 50 times per fly. The stimulus was rendered in real-time using Panda3D, an open source game engine, and Python 2.7.

Data Analysis

We analyzed the data as described previously [S5]. Briefly, optical tracking sensors were equipped with lens and aperture systems to focus on the sphere behind the fly. The tracking data were processed at 4 kHz internally, read out via a USB interface and processed by a computer at 100 Hz. This allowed real-time calculation of the instantaneous rotation axis of the sphere. We resampled the rotation traces to 20Hz for further processing and applied a first-order low pass filter with a time constant of 100ms to each trace. For all flies, we manually selected 20 consecutive trials out of the 50 available that fulfilled the following criteria: First, the temperature was at a stable 34°C . Second, the average turning tendency of the fly was approximately 0° s^{-1} . Third, the average forward velocity of the fly was at least 5mm s^{-1} , indicating a visually responsive state. Flies were selected without blinding. Application of the criteria excluded, on average, 20% of all measured flies. For further processing, we subtracted responses for the two symmetrical edge directions in order to reduce the impact of walking asymmetries. Trials were then averaged. For statistical purposes, we calculated the turning tendency of each fly for each velocity condition as the mean of the turning response between 3s (walking onset) and 7s (stimulus offset). Other evaluation time frames produced qualitatively equivalent results. All data analysis was performed using Python 2.7 and the NumPy library.

Modeling

Modeling the motion detection pathway followed Eichner et al., 2011 [S6]. Briefly, stimuli were represented as brightness values between 0 and 1 at the level of 40x40 photoreceptors with an angular resolution of 5° at a temporal resolution of 10 ms. Signals of lamina cells L1 and L2 were calculated by high-pass filtering (time-constant 250 ms) the photoreceptor input plus 10% of their DC level. The ON (L1) signal was obtained by half-wave rectifying the signal at a threshold of 0, the OFF (L2) signal was inverted and half-wave rectified at a threshold of 0.05. These signals were then processed by separate ON- and OFF-motion detectors. Within each detector (Figure 1A), the output signal of the lamina cell at one location was low-pass filtered ($\tau = 50$ ms) and subsequently multiplied with the instantaneous signal of the lamina cell from the adjacent location. This was done twice in a mirror-symmetrical way and the results subtracted from each other. Finally, the output signals of all ON- and OFF-motion detectors were added.

Statistics

Throughout the paper we tested for statistical significance by using a two-sided Student's t-test followed by a Benjamini-Hochberg correction (* p<0.05). Detailed statistics are documented in [Table S2](#).

Supplemental References

- S1. Yu, J.Y., Kanai, M.I., Demir, E., Jefferis, G.S., and Dickson, B.J. (2010). Cellular organization of the neural circuit that drives *Drosophila* courtship behavior. *Curr Biol* **20**, 1602-1614.
- S2. Nern, A., Pfeiffer, B.D., and Rubin, G.M. (2015). Optimized tools for multicolor stochastic labeling reveal diverse stereotyped cell arrangements in the fly visual system. *PNAS* **112**, 2967-2976.

- S3. Bahl, A., Ammer, G., Schilling, T., and Borst, A. (2013). Object tracking in motion-blind flies. *Nat Neurosci* *16*, 730-738.
- S4. Clark, D.A., Bursztyn, L., Horowitz, M.A., Schnitzer, M.J., and Clandinin, T.R. (2011). Defining the computational structure of the motion detector in *Drosophila*. *Neuron* *70*, 1165-1177.
- S5. Maisak, M.S., Haag, J., Ammer, G., Serbe, E., Meier, M., Leonhardt, A., Schilling, T., Bahl, A., Rubin, G.M., Nern, A., et al. (2013). A directional tuning map of *Drosophila* elementary motion detectors. *Nature* *500*, 212-216.
- S6. Eichner, H., Joesch, M., Schnell, B., Reiff, D.F., and Borst, A. (2011). Internal structure of the fly elementary motion detector. *Neuron* *70*, 1155-1164.